General 3D Lumped Thermal Model with Various Boundary Conditions for High Power IGBT Modules

Bahman, Amir Sajjad; Ma, Ke; Blaabjerg, Frede

Published in:
Proceedings of the 31st Annual IEEE Applied Power Electronics Conference and Exposition (APEC)

DOI (link to publication from Publisher):
10.1109/APEC.2016.7467882

Publication date:
2016

Document Version
Accepted author manuscript, peer reviewed version

General 3D Lumped Thermal Model with Various Boundary Conditions for High Power IGBT Modules

Amir Sajjad Bahman, Ke Ma, Frede Blaabjerg
Center of Reliable Power Electronics (CORPE)
Department of Energy Technology, Aalborg University, 9220 Aalborg, Denmark
asb@et.aau.dk, kema@et.aau.dk, fbl@et.aau.dk

***Abstract*— Accurate thermal dynamics modeling of high power Insulated Gate Bipolar Transistor (IGBT) modules is important information for the reliability analysis and thermal design of power electronic systems. However, the existing thermal models have their limits to correctly predict these complicated thermal behaviors in the IGBTs. In this paper, a new three-dimensional (3D) lumped thermal model is proposed, which can easily be characterized from Finite Element Methods (FEM) based simulation and acquire the thermal distribution in critical points. Meanwhile the boundary conditions including the cooling system and power losses are modeled in the 3D thermal model, which can be adapted to different real field applications of power electronic converters. The accuracy of the proposed thermal model is verified by experimental results.**

Keywords—Insulated gate bipolar transistors, Thermal modeling, Boundary conditions, Finite element method, Reliability, Power electronic converters.

I. INTRODUCTION

Insulated Gate Bipolar Transistor (IGBT) modules are widely applied in power electronic conversion systems especially in high power application like renewable energy systems, traction industries and HVDC [1]. Since industries demand for higher power densities, more integrated packaging, and cost saving, the risk of failures and reliability of the power electronics become more crucial. Consequently, thermal management of power semiconductors finds more importance due to increased heat generation inside the devices [2]. The first step in thermal management of the power semiconductor devices is to identify accurate and detailed temperature information in critical locations by using compact thermal models [3]. However, accurate thermal modeling of high power IGBT modules is of great challenges due to several physical and operational factors. The physical factors are related to geometries – e.g. size, thickness and positon of the semiconductor chips – as well as thermal properties of materials used in different layers of the IGBT module. These factors lead to uneven thermal distribution among the chips as well as the sub-layers inside the IGBT module due to thermal coupling effects [4]. On the other hand, operational factors include those related to long-term mission profiles and thermal dynamics, which are crucial for lifetime calculation and thermal design/management of high power module. In many lifetime models, temperature cycles in critical locations such as junction and solder layers are important factors to be identified for a reliable design of IGBT modules [5].

Currently, various compact thermal models have been introduced. The first group of thermal models is based on one dimensional lumped RC networks, e.g. Cauer or Foster type models. Typically the equivalent thermal circuit consists of several RC pairs to identify the dynamics of the device temperatures in respect to the power losses injected to the semiconductor chips [6]. Conventionally, Cauer or Foster thermal networks are given by the manufacturer in the IGBT module datasheet. These thermal models are all based on a one dimensional (1D) modeling approach of the heat conduction and can be used for a rough and fast calculation of junction temperature. However, they cannot be used for studying the three dimensional (3D) heat spreading effects to come up with accurate temperatures in different locations. The other group of thermal models is based on analytical solutions to the heat equation. Due to the complexity of the thermal system, Finite Element Method (FEM) or Finite Difference Method (FDM) simulations have been used to calculate the 3D thermal behaviors in power module [7]-[9]. However, these methods are not efficient for long-term mission profile-based analysis of IGBT modules since they demand large computational cost and may also lead to divergence for high dynamic operation.

Apart from thermal dynamics, variation of boundary conditions is neglected in the thermal models, which are inevitable on the thermal analysis of IGBT modules. The boundary conditions in term means a set of conditions that is required to be satisfied at all or one part of the boundaries of a design geometry in which a set of differential equations is to be solved [10]. In an IGBT module, boundary conditions consist of heat sources i.e. power losses in the semiconductor chips and heat sink i.e. cooling system [11]. On the other hand, in a reliable design of high power IGBT modules, it is important to evaluate the dynamic thermal behavior with real load profiles associated with e.g. renewable or automotive applications. For this reason, a circuit simulator has the benefits of fast simulation for given load profiles.

In the this paper, a method to transform the boundary conditions from the FEM environment to a circuit simulator is given, which has benefits of FEM's accuracy and circuit simulator speed. A generic 3D thermal model will be introduced with flexible RC elements to be used for different heating and cooling conditions, and is able to calculate temperatures at different locations and layers of the IGBT. The introduced thermal model is verified by thermography measurements from a power cycling test setup.

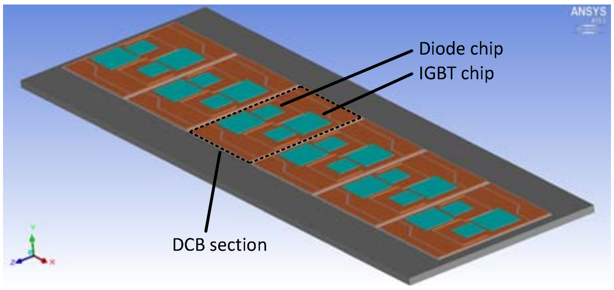

Fig. 1. Schematic of high power IGBT module modeled in ANSYS Icepak for FEM analysis.

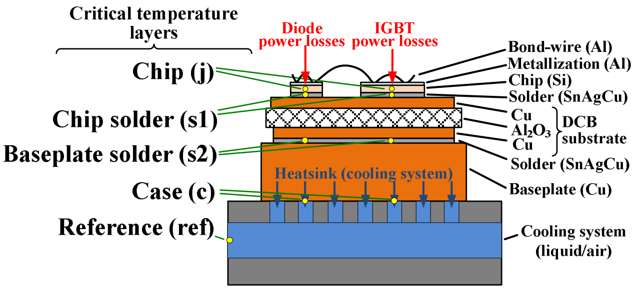

Fig. 2. IGBT module layers and boundary conditions of high power IGBT module modeled in ANSYS Icepak for FEM analysis.

II. The Proposed Three-Dimensional Thermal Network

A high power IGBT module consisting 6 full-bridge Direct Copper Bonded (DCB) sections connected in parallel is shown in Fig. 1. The materials of IGBT module and boundary conditions for thermal analysis are shown in Fig. 2. There are two boundary conditions in this case study, one is at the chip junction as the heat source (power losses), and the other one at the bottom of the baseplate as the cooling capability (heat sink/cooling system). The thermal characteristics for the materials used in the IGBT module under study are given in Table I. It is noted that the conductivity of some materials is set to be temperature dependent according to [12]. For simplicity of analysis it is assumed that the IGBT module is adiabatic from the top and the lateral surfaces and therefore all generated heat is dissipated in the cooling system.

When the model is ready to be used in the FEM environment, specific indexes should be defined to identify the boundary condition related effects on transient thermal behavior of IGBT module. Therefore, the transient thermal impedance curves are defined in the design geometry of IGBT module. In dynamic operation, the temperature difference between every two points is calculated using the transient thermal impedance curve, $Z_{th}(t)$. The transient thermal impedance between two points is explained by

$$Z_{th(a-b)}(t) = \frac{T_a(t) - T_b(t)}{P} \tag{1}$$

where $T_a(t)$ and $T_{b(t)}$ are transient temperatures in two points and P is the power dissipation, which is generated in the

TABLE I. IGBT Module Material Thermal Properties

Material	Density kg/m^3	Specific heat $J/(kg \cdot K)$	Conductivity $W/(m \cdot K)$ Temp. (°C)	Conductivity
Silicon (Si)	2330	705	0.0 100.0 200.0	168 112 82
Copper (Cu)	8954	384	0 100 200	401 391 389
Al_2O_3	3890	880	all	35
SnAgCu	7370	220	all	57

device. To derive the thermal impedances, a single square power pulse with amplitude P is applied to a heat source in the power module (IGBT chip or diode chip) until the junction temperature reaches the steady state. Then, by dividing the temperature difference between each two neighboring region to power loss, a transient thermal impedance curve is obtained. To derive the transient thermal impedances, a step response analysis is implemented in FEM simulation [13]. The curves are fitted into a finite number of exponential terms by

$$Z_{th(a-b)}(t) = \sum_{i=1}^{n} R_{thi}.(1 - e^{-t/\tau_{thi}}) \tag{2}$$

where R_{thi} is thermal resistance, τ_{thi} is time constant which equals to $R_{thi}*C_{thi}$ and n is the number of exponential terms. Commonly, four exponential terms are enough to fit $Z_{th(a-b)}(t)$ with enough accuracy for the intended application. The number of exponential terms determines the number of RC pairs in the RC thermal network. The details of the extraction process have been explained in [13]. The thermal network, which is used in this work is a Foster network and is widely used by industry due to the simplicity of extraction of parameters.

Most of the IGBT module failures occur due to bond wire lift-off or solder crack, so the temperature profiles in these locations are critical [14]. Thus, the IGBT module is divided vertically into four sections and the thermal impedance curves are derived between layers to study the transient thermal behavior of IGBT module. These sections are shown in Fig. 2. Moreover, to study the thermal stress on bond wire heel locations, temperatures at different points on the chip surface are required to be identified. Based on the described critical temperature locations, a 3D thermal network is extracted, which includes all the mentioned nodes, different temperature locations on material layers, heat sources, heat sink and thermal coupling effects from other heat sources. The schematic of the 3D thermal network is shown in Fig. 3.

III. Characterization and Modeling of Boundary Conditions for the Thermal Analysis

In order to understand the importance of the boundary condition effects in thermal impedance of IGBT module, the cooling system variations are modeled by FEM simulations and temperature responses are extracted in the corresponding points in the 3D thermal network. To represent the capability

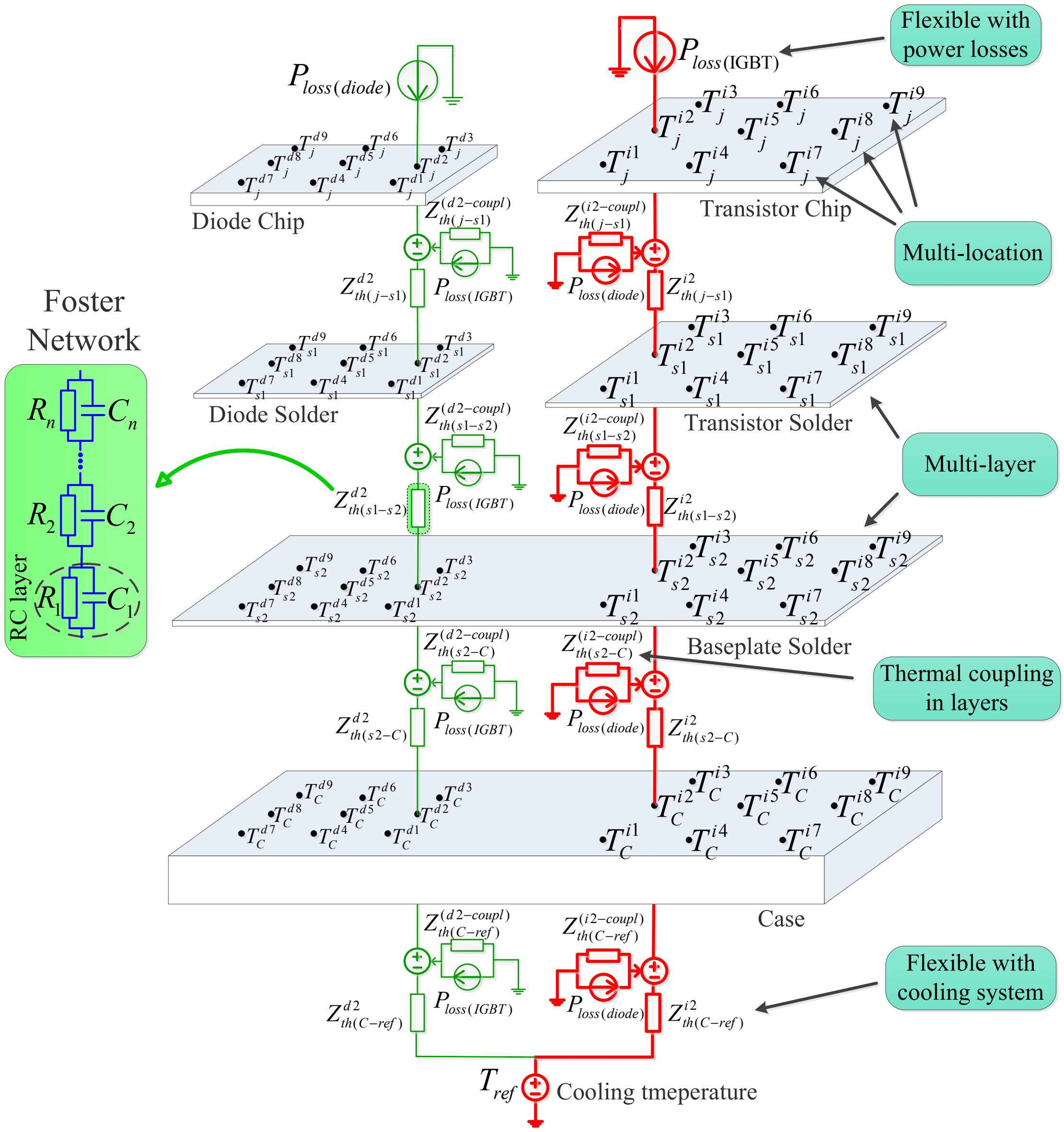

Fig. 3. 3D thermal network from chip (junction) to reference (cooling temperature).

of the fluid cooling systems, different cooling mechanisms are considered in the heatsink. For each cooling mechanism, the equivalent heat transfer coefficient, *htc*, of the cooling system is extracted and modelled as a thick plate beneath the baseplate. The equivalent *htc* is a measure, which stands for the amount of heat, which is transferred by convection between a solid and a fluid [12]. The *htc* in concept is the proportionally coefficient between the heat flux and the temperature difference between the solid and fluid:

$$htc = \frac{q}{\Delta T}\,[W/m^2 \cdot K] \tag{3}$$

where q is the amount of heat, which is transferred between two materials (heat flux) and ΔT is the temperature difference between the solid surface and surrounding fluid area. The heat flux, q, in turn is defined as the thermal power (or power losses in the IGBT module) per unit area:

$$q = \frac{d\dot{Q}}{dA}\,[W/m^2] \tag{4}$$

where A is defined as the effective area for heat dissipation of the heatsink. Moreover, the thermal resistance between the IGBT module and the heatsink, $R_{th(c\text{-}ref)}$, can be defined based on the definition of heat transfer coefficient

$$R_{th(c-ref)} = \frac{1}{htc \cdot A}\,[K/W] \tag{5}$$

From eq. (5), it can be seen that a higher *htc* leads to a smaller R_{th}. With a *htc*, heat flux in the power module is more localized beneath the IGBT chips that lead to a smaller heat spreading specially in the baseplate. This will reduce the effectiveness of the baseplate area in spreading the heat dissipation; so the temperature difference between the junction

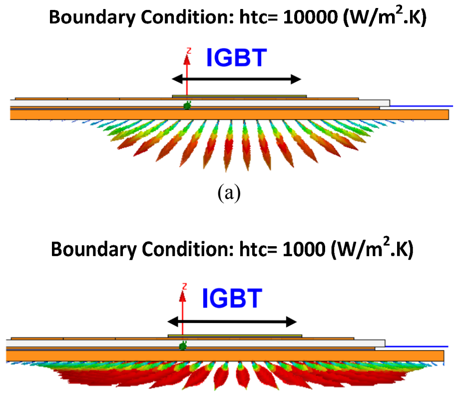

(a)

(b)

Fig. 4. Heat flux distribution in a power module for heat transfer coefficient: (a) 10000 W/m^2·K, (b) 1000 W/m^2·K.

TABLE II. HEAT TRANSFER COEFFICIENTS FOR SOME COMMON FLUIDS (W/m^2·K)

Free convection-Air	5-25
Free convection-Water	20-100
Forced convection-Air	10-200
Forced convection-Water	50-10000
Boiling water	3000-100000
Condensing water vapor	5000-10000

and case will be increased. This phenomenon is shown in Fig. 4. As listed in [12], the equivalent *htcs* can vary from *10 W/m^2·K* for natural convection systems to *10^5 W/m^2·K* for phase change cooling systems. Typical values for those cooling systems are listed in Table II. With the method described in section II, the transient thermal impedance curves are extracted for different *htcs*. The *htcs* within the ranges of *3000<htc<100000 W/m^2·K* are used in this paper, which represents reasonable cooling conditions for the IGBT module under study. The transient thermal impedances under different *htcs* are shown in Fig. 5. As it is shown, the most influenced thermal impedance is the section from case to reference (cooling fluid temperature) due to its closer distance to the heatsink.

On the other hand, the effect of a hot plate (fixed case temperature) variation beneath the baseplate on thermal impedance of IGBT module is studied. To model the fixed case temperature, in FEM environment, a thick plate is placed under the baseplate and boundary condition between the baseplate and wall is set to a very high *htc* (close to infinite). The reference temperature at the back of thick plate is then changed to have the same case temperature as the hot plate should perform. In this study, the case temperature is varied in the range of 20°C to 120°C. The results are shown in Fig. 6. As it is seen the most affected section is the junction to chip solder. The reason originates from thermal blocking behavior of the case surface of the device, which prevents the heat to be dissipated in the heatsink. So, the heat generated in the chip does not propagate to the lower layers and tends to be remained in the upper layers.

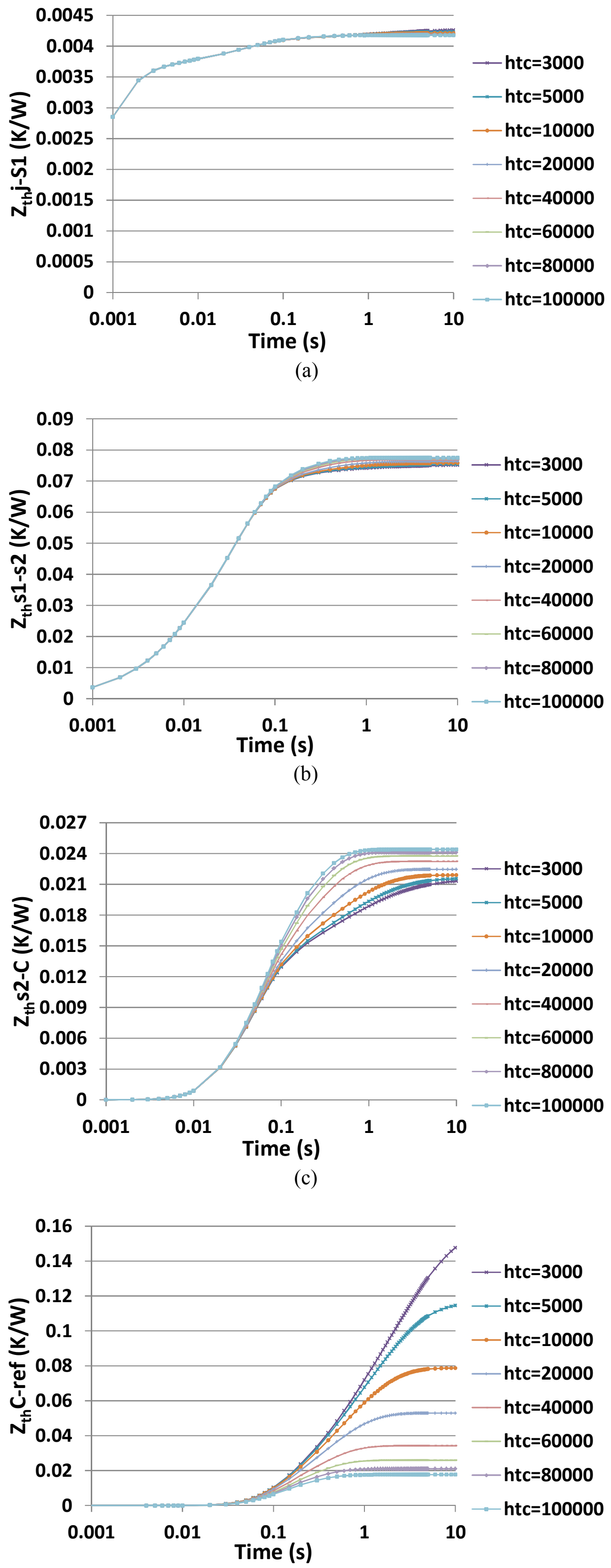

(a)

(b)

(c)

(d)

Fig. 5. Transient thermal impedances in different layers for various **cooling systems (*htc* in W/m^2·K)**. (a) junction to chip solder, (b) chip solder to baseplate solder, (c) baseplate solder to case, (d) case to reference.

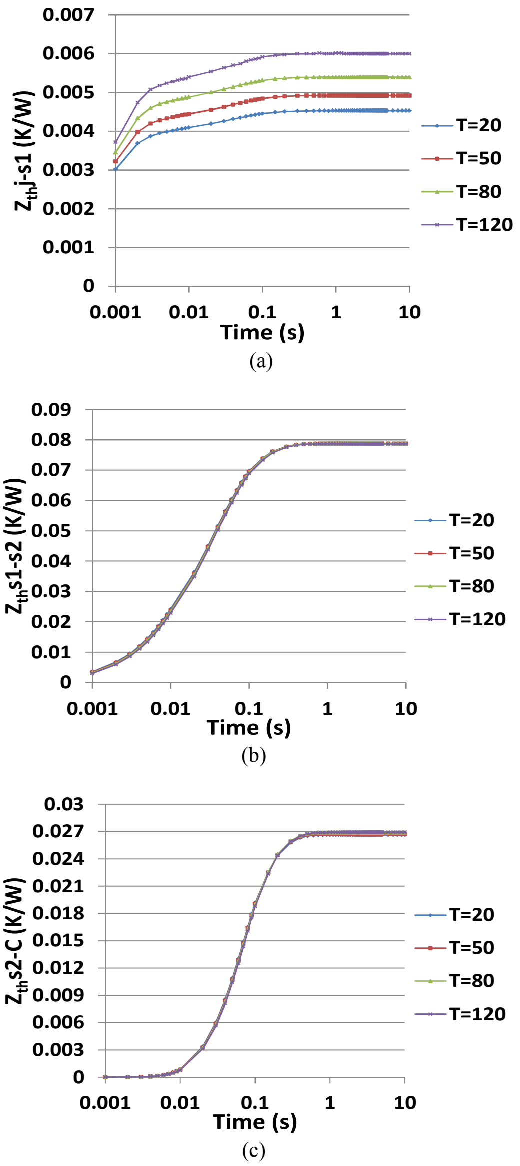

Fig. 6. Transient thermal impedances in different layers for various **hotplates (*T* in °C)**. (a) junction to chip solder, (b) chip solder to baseplate solder, (c) baseplate solder to case, (d) case to reference.

IV. Transformation of Boundary Conditions from FEM Model to Lumped RC Network

It was discussed in section I that FEM simulations can be used in the case of short-term load profiles. For longer load profiles (e.g. 1 day or 1 year for a complete mission profile), FEM simulation will be too time-consuming and demands for high computational facilities. Therefore, simplified thermal models are needed to be used in circuit simulators. But, in circuit simulators it is very hard to model the effect of boundary conditions in the compact thermal model. The boundary conditions need to be translated from FEM to circuit simulator in order to develop a more general thermal model. This is possible to implement by using a step response analysis for different boundary conditions in FEM. By using a step response analysis, the transient thermal impedance curves are extracted and mathematically fitted to a 3D thermal network. As shown in Fig.3, Foster networks in the 3D thermal network can vary from one RC layer to multiple RC layers depending on the accuracy of the curve-fitting. For simplicity of modeling of the boundary conditions, one RC layer is used in this work.

The RC element values in respect to the different cooling systems are shown in Fig. 7. For a higher accuracy of the thermal model, the thermal coupling branches are connected to the main branch as controlled voltage sources. As described in section II, the highly affected regions are from baseplate solder to case and from case to reference. The variation is mathematically curve fitted to find the generic model for various cooling mechanisms. In the given curves, the horizontal axis shows different *htc*s (different cooling conditions) and the vertical axis shows the respected thermal resistance and thermal capacitance values. The curve fitted linear mathematical model and respected R-squared values are also shown beside the curves. For all cases, the R-squared values are at least 0.9 for a better accuracy of the curve-fitting [15].

The generic thermal models for variation of case temperatures and power losses follow the same approach. The schematic of one branch of 3D thermal network (highlighted in red in Fig. 3) with a variation of cooling system is also shown in Fig. 8. As it is seen, the RC elements in the regions which are not varied by the cooling system are shown as constant values. By variation of the RC elements in the 3D thermal network, a flexible thermal network is developed in which RC elements are dependent on the boundary conditions. In other words, by the presented approach, thermal model of IGBT module can get feedback from the boundary conditions in transient operation, and calculate accurately the temperatures at different locations with a very high simulation speed. The parameters needed to construct this network are the geometries and materials of the IGBT module, the equivalent *htc* that can be extracted by Computational Fluid Dynamics (CFD) simulations of the real cooling system or rough values given in heat transfer handbooks, the power loss level that module will be used, the ambient temperature and the case temperature. Of course, the 3D thermal network can be constructed by the parameters given in one condition; however, to extract a generic thermal model, RC elements can be modeled as variable parameters for a few possible operating conditions.

V. Experimental Verification

The boundary-dependent thermal model is tested in a real power cycling operation. For this purpose, an experimental setup is established. The IGBT module is loaded with a three-phase DC-AC two-level Voltage Source Converter (2L-VSC). The detailed converter specifications are listed in Table III. The fundamental frequency of the converter is set to 6 Hz, which is usual in reliability power cycling tests [16]. A black painted, opened IGBT module is being monitored by an IR camera (Fig. 9). The IGBT module is mounted on a direct liquid cooling system where the liquid cooling temperature and flow rate can be controlled for each experiment.

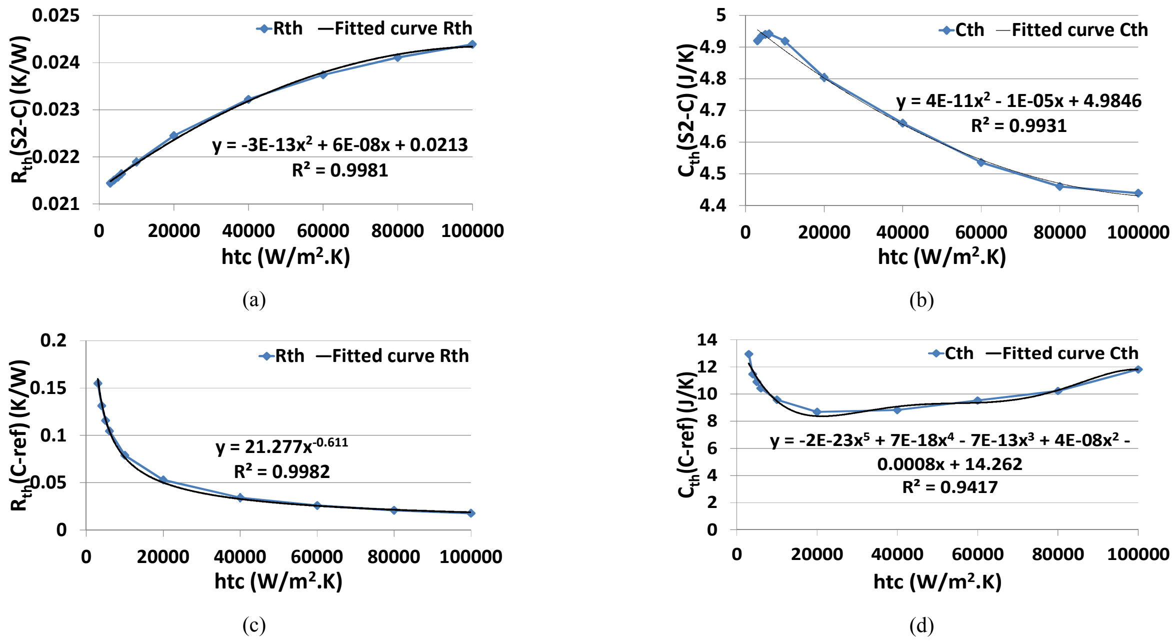

Fig. 7. Curve fitted thermal resistance and thermal capacitance for various **cooling systems**. (a) baseplate solder to case thermal resistance, (b) baseplate solder to case thermal capacitance, (c) case to reference thermal resistance, (d) case to reference thermal capacitance.

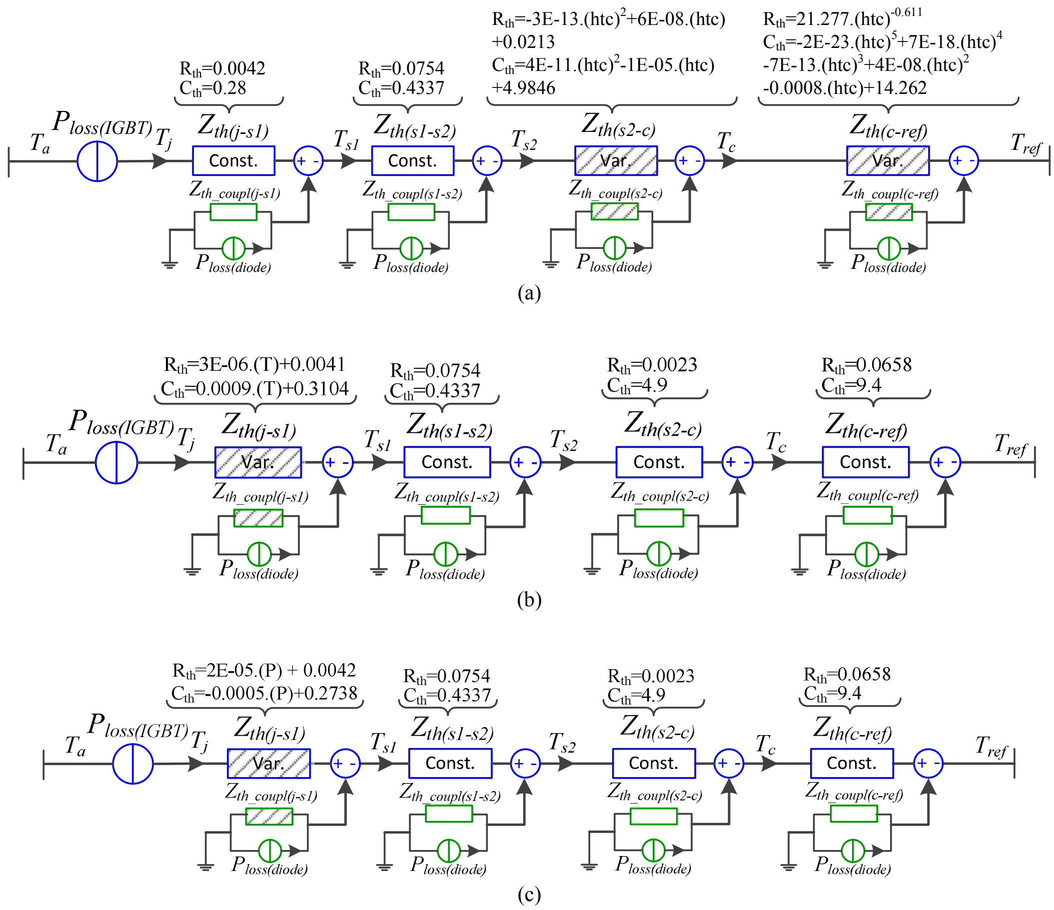

Fig. 8. Schematics of one branch of 3D thermal network (highlighted in red in Fig. 3) with different boundary conditions. (a) variation of fluid cooling system, (b) variation of hotplate, (c) variation of power losses.

TABLE III. PARAMETERS OF THE TWO LEVEL VOLTAGE SOURCE CONVERTER

DC bus voltage V_{dc}	450 V
Rated load current I_{load}	variable up to 900 A (peak)
Fundamental frequency f_o	6 Hz
Switching frequency f_{sw}	2.5 kHz
Filter inductor L_l	350 µH
IGBT module	1700V/1000A

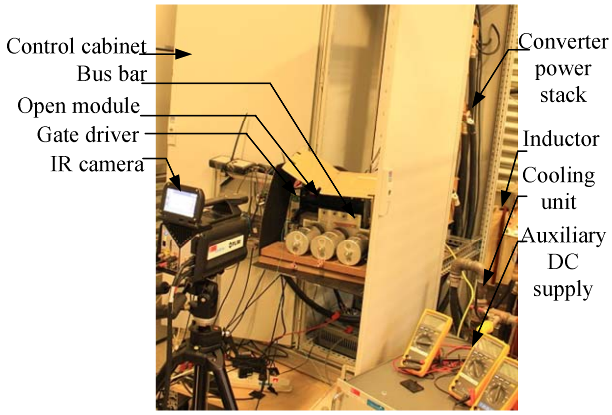

Fig. 9. Test setup featured with the infra-red camera.

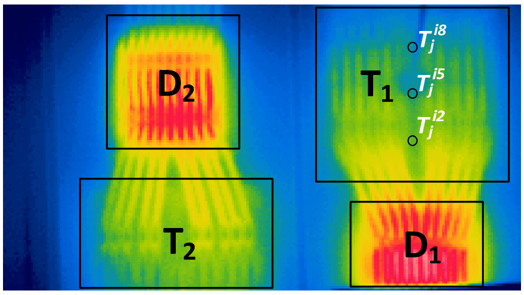

Fig. 10. Thermographical picture of one DCB section at the surface of IGBT module.

The cooling system is able to dissipate the heat from the IGBT module homogenously [17]. The infrared thermal image of one DCB section of the IGBT module is shown in Fig. 10. To validate the presented model, similar monitoring points as in the 3D thermal network are considered on the surface of the IGBT chip and the diode chip. The monitoring points should be considered between the bond-wires and be on the surface of the chips to prevent false temperature monitoring of the bond-wires.

In the simulation environment (e.g. PLECS), the same converter topology is established and the power losses are applied into the IGBT chips and diode chips. The peak of the load current, $I_{load(peak)}$, is fixed to *500 A*, cooling liquid flow rate, $\dot{V}$, is set to $5\ m^3/hr$ and cooling liquid temperature , $T_{cooling}$, is set to 45°C. For the cooling system, the equivalent *htc* is set to 7000 $W/m^2{\cdot}K$ as suggested by the manufacturer of

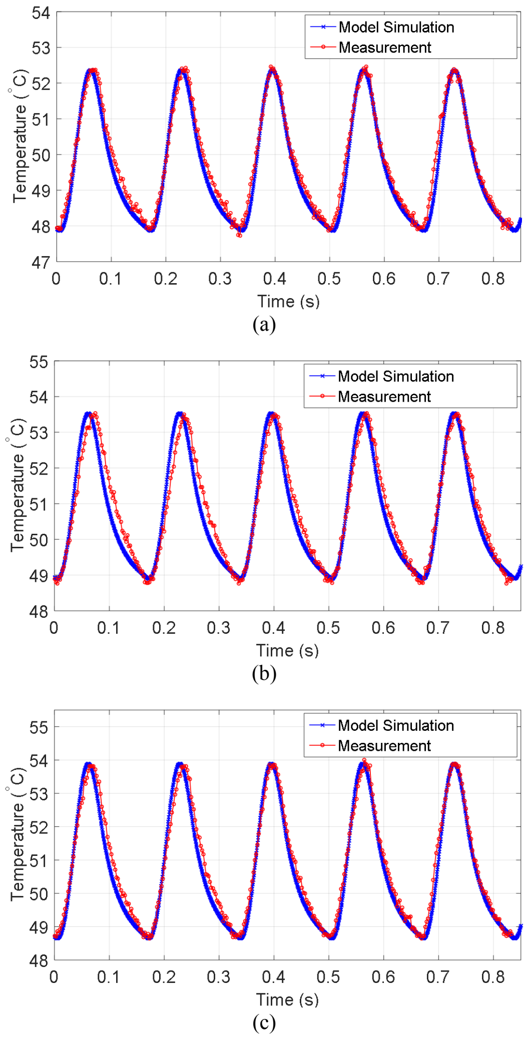

Fig. 11. Comparison of junction temperatures by the thermal model simulation and measurement in $I_{load(peak)}=500A$, $\dot{V}=5m^3/hr$, and $T_{cooling}=45°C$. (a) i_2, (b) i_5, and (c) i_8 (see Fig. 3).

the cooling system for the mentioned flow rate. The equivalent *htc* of the cooling system is dependent on the liquid flow rate and geometries of cooling system and can be calculated by CFD simulations. Since it is difficult to access the accurate power losses in the experimental setup, the power losses used in the thermal model are calculated based on the IGBT module datasheet, and power losses applied to the thermal model were adjusted in such a way to achieve the same case temperature as the experimental setup. However, the loss is only adjusted within ±10%, which is a reasonable range for the loss estimation error by datasheet. The junction and case temperatures are extracted for three different points: i_2, i_5 and i_8 (see Fig. 3). The results are shown in Fig. 11. The boundary-dependent 3D thermal model accurately calculates the same junction temperatures as seen in the experimental results. It should be mentioned that the main feature in the presented thermal model is its high accuracy in the calculation of steady-state peak-to-peak temperature, ΔT, and maximum temperature, T_{max}, of junction temperature, which are the main factors in life-time models for IGBT modules. For both parameters, the thermal model shows less than 2% error in steady-state compared to the experimental results. To be ensured about the validity of the thermal model on the other boundary conditions, the next validation is implemented for these conditions: $I_{load(peak)}=700\ A$, $\dot{V}=1\ m^3/hr\ (htc=3000\ W/m^2{\cdot}K)$, and $T_{cooling}=34^{\circ}C$. Results are shown in Fig. 12 for temperature monitoring points: i_2, i_5 and i_8. Similarly to the previous case, thermal model results are consistent with the experimental results in both steady-state ΔT and T_{max}.

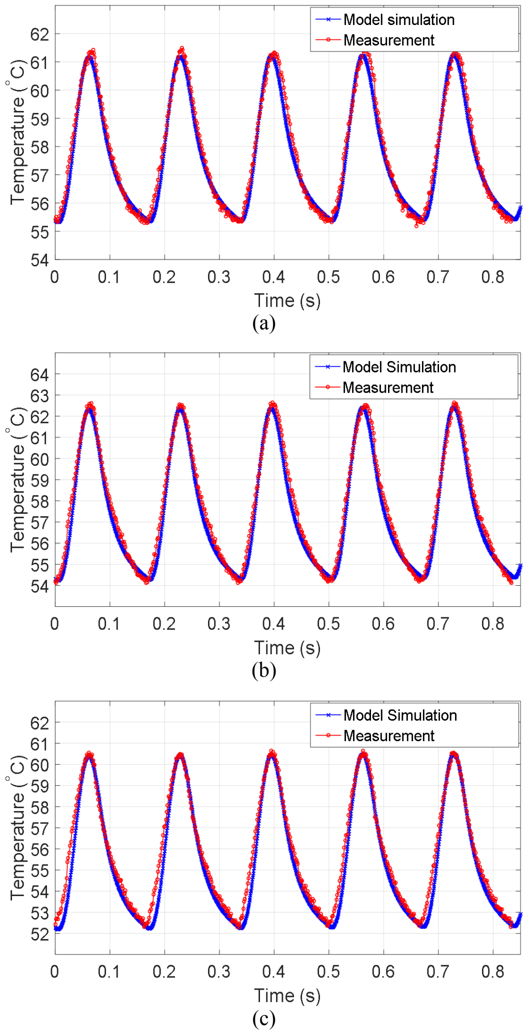

Fig. 12. Comparison of junction temperatures by the thermal model simulation and measurement in $I_{load(peak)}=700A$, $\dot{V}=1m^3/hr$, and $T_{cooling}=34°C$. (a) i_2, (b) i_5, and (c) i_8 (see Fig. 3).

VI. Conclusions

In this paper, a simplified boundary-dependent thermal model for high power IGBT modules has been presented. The boundary conditions, which were applied in the model, are the heat source (power losses) and the heatsink (cooling system). The presented thermal model is a generic RC lumped network model, which is controlled by the variation of boundary conditions. It has been proved that by changing in the cooling system, the lower layers closer to the heatsink are more affected. So, the baseplate solder layer is more stressed and is face to reliability issues. By translation of the FEM thermal model to a circuit simulator a boundary-dependent 3D thermal network has been extracted, which can estimate detailed and accurate temperatures of the power module in different locations and layers. This thermal model has the benefits of FEM accuracy and circuit simulator speed and it can be used for accurate and detailed temperature estimation in real operating conditions. The simulated temperature profiles can be used for accurate life-time estimation of the IGBT module for long-term mission profiles.

References

[1] S. Yantao, and W. Bingsen, "Survey on Reliability of power electronic systems," *IEEE Trans. Power Electron.*, vol. 28, no. 1, pp. 591-604, Jan. 2013.

[2] H. Wang, M. Liserre and F. Blaabjerg, "Toward reliable power electronics: challenges, design tools, and opportunities," *IEEE Ind. Electron. Mag.*, vol. 7, no. 2, pp.17-26, Jun. 2013.

[3] G. Moreno, S. Narumanchi, K. Bennion, S. Waye, and D. DeVoto, "Gaining Traction: Thermal Management and Reliability of Automotive Electric Traction-Drive Systems," *IEEE Electrification Mag.*, vol.2, no.2, pp.42-49, June 2014.

[4] A. S. Bahman, K. Ma and F. Blaabjerg, "Thermal mpedance model of high power IGBT modules considering heat coupling effects," in *Proc. Electron. App. Conf. Expo. (PEAC)*, 2014, pp.1382-1387.

[5] H. Wang, M. Liserre, F. Blaabjerg, P. de Place Rimmen, J.B. Jacobsen, T. Kvisgaard, J. Landkildehus, "Transitioning to Physics-of-Failure as a Reliability Driver in Power Electronics," *IEEE J. Emerg. Sel. Topics Power Electron.* , vol.2, no.1, pp.97-114, March 2014.

[6] ABB, *Thermal design and temperature ratings of IGBT modules*, App. Note 5SYA 2093-00, pp. 5-6.

[7] D. Cottet, U. Drofenik, and J.-M. Meyer, “A systematic design approach to thermal-electrical power electronics integration,” in *Proc. Electron. Syst.-Integr. Technol. Conf.*, 2008, pp. 219–224.

[8] T. Kojima, Y. Yamada, Y. Nishibe, and K. Torii, “Novel RC compact thermal model of HV inverter module for electro-thermal coupling simulation,” in *Proc. Power Convers. Conf. (PCC)*, 2007, pp. 1025–1029.

[9] S. Carubelli, and Z. Khatir, “Experimental validation of a thermal modelling method dictated to multichip power modules in operating conditions,” *Microelectron. J.*, vol. 34, pp. 1143–1151, Jun. 2003.

[10] D. V. Hutton, *Fundamentals of Finite Element Analysis*, Freiburg, Germany: Mcgraw-Hill, 2003.

[11] M. Ibrahim, S. Bhopte, B. Sammakia, B. Murray, M. Iyengar, and R. Schmidt, "Effect of Transient Boundary Conditions and Detailed Thermal Modeling of Data Center Rooms," *IEEE Trans. Compon. Packag. Manuf. Technol.*, vol.2, no.2, pp.300-310, Feb. 2012.

[12] J. H. Lienhard IV, and J. H. Lienhard V, *A Heat Transfer Textbook*, 4th ed. Englewood Cliffs, New Jersey: Prentice-Hall Inc., 2013.

[13] A. S. Bahman, K. Ma, P. Ghimire, F. Iannuzzo, and F. Blaabjerg, "A 3D Lumped Thermal Network Model for Long-term Load Profiles Analysis in High Power IGBT Modules," *IEEE J. Emerg. Sel. Topics Power Electron.*, to be published.

[14] N.Y.A. Shammas, “Present problems of power module packaging technology,” *Microelectron. Rel.*, vol. 43, pp. 519-527, April 2003.

[15] MATLAB version 8.1.0.604, The MathoWorks Inc., 2013.

[16] P. Ghimire, A. R. de Vega, S. Beczkowski, B. Rannestad, S. M. -Nielsen, and P. Thogersen, "Improving Power Converter Reliability: Online Monitoring of High-Power IGBT Modules," *IEEE Ind. Electron. Mag.*, vol.8, no.3, pp.40-50, Sept. 2014.

[17] K. Olesen, R. Bredtmann, and R. Eisele, ”ShowerPower® New Cooling Concept”, in *Proc. PCIM’2004*, 2004. pp.1-9.